JOC Article

Arteminolides B, C, and D, New Inhibitors of Farnesyl Protein Transferase from *Artemisia argyi*

Seung-Ho Lee, Hyae-Kyeong Kim, Jeong-Min Seo, Hyun-Mi Kang, Jong Han Kim, Kwang-Hee Son, Heesoon Lee,† and Byoung-Mog Kwon*

Korea Research Institute of Bioscience and Biotechnology, P.O. Box 115, Yusung, Taejon 305-600, Republic of Korea, and College of Pharmacy, Chungbuk National University, Cheongju 360-763, Republic of Korea

Jongheon Shin and Youngwan Seo

Marine Natural Products Laboratory, Korea Ocean Research & Development Institute, P.O. Box 29 Ansan, Seoul 425-600, Republic of Korea

kwonbm@kribb.re.kr

Received April 29, 2002

Arteminolides B−D (**2**−**4**), new farnesyl protein transferase inhibitors, were isolated together with a known arteminolide A (**1**) and new regioisomers (**5**−**7**) of the compounds from the aerial parts of *Artemisia argyi*. Structures of these compounds were elucidated by spectroscopic methods and chemical conversion. Arteminolides inhibited the farnesyl protein transferase with IC_{50} values of 0.7−1 μM, while the regioisomers **5**−**7** were inactive. In addition, it was proved that the exocyclic double bond of sesquiterpene lactone did not affect the inhibitory activity of arteminolide. The effects of compound **2** on H-Ras processing and cellular growth in H-*ras*-transformed cells were also evaluated.

Introduction

The currently known function for Ras in signal transduction is in mediating the transmission of signals from external growth factors to the cell nucleus. Mutated forms of this GTP-binding protein are found in 30% of human cancers with particularly high prevalence in colon and pancreatic carcinomas.[1] Ras proteins are produced as cytoplasmic precursor proteins and require their association with the plasma membrane to acquire full biological activity.[2] This is achieved by posttranslational modifications including the farnesylation onto cysteine 186 at the C-terminal of Ras by farnesyl protein transferase (FPTase). Treatment of Ras-transformed cells with FPTase inhibitors results in selective suppression of Ras-dependent oncogenic signaling. This includes the inhibition of Ras processing, which results in a decrease in the relative amount of fully processed Ras, the progressive, dose-dependent cytoplasmic accumulation of unprocessed Ras and inactive Ras-Raf complexes, inhibition of the Ras-induced constitutive activation of MAPK, and decreased transcriptional activities of both c-Jun and Elk-1.[3] Treatment of tumor cells with FPTase inhibitors also induces the G1 block and apoptosis by upregulating Bax and Bcl-xs expression and by activating caspases.[4] Synergy of FPTase inhibitors with established anticancer treatments such as radiation and chemotherapeutic treatment was recently reported. Agents that prevent microtubule depolymerization, such as taxol and epothilones, act synergistically with FPTase inhibitors to block cell growth. FPTase inhibitors cause increased sensitivity to induction of the metaphase block by taxol and epothilones.[5] In addition, FPTase inhibitors have been shown to increase the radiosensitivity of human tumor cells with activating mutations of *ras* oncogenes.[6]

FPTase inhibitors have also been shown to inhibit the growth of Ras-induced tumors in mouse xenograft models and, more dramatically, in transgenic mouse models. Recent work has demonstrated that specific inhibitors of the FPTase might be interesting chemical leads to develop effective therapeutic agents for the treatment of cancer.[7] Many strategies have been used to develop FPTase inhibitor, including screening of natural products and rational design based upon the substrates of the farnesylation reaction.

We have continued screening for potent inhibitors of FPTase from herbal medicines and recently reported

* Address correspondence to this author at the Korea Research Institute of Bioscience and Biotechnology.
† College of Pharmacy, Chungbuk National University.

(1) Yimin, Q.; Sebti, S. M.; Andrew, D. H. *Biopolymers* **1997**, *43*, 25−41.
(2) Christoph, W. M.; Morgan, M. A.; Lothar, B. *Blood* **2000**, *96*, 1655−1669.
(3) Cox, A. D.; Garcia, A. M.; Westwick, J. K.; Kowalczyk, J. J.; Lewis, M. A.; Brenner, D. A.; Der, C. J. *J. Biol. Chem.* **1994**, *269*, 19203−19206.
(4) Lebowitz P. F.; Sakamuro, D.; Prendergast, G. C. *Cancer Res.* **1997**, *57*, 708−713.
(5) Mark, M.; Moasser M. M.; Sepp-Lorenzio, L.; Kohl, N. C.; Oliff, A.; Balog, A.; Su, D. S.; Danishefsky, S. J.; Rosen, N. *Proc. Natl. Acad. Sci. U.S.A.* **1998**, *95*, 1369−1374.
(6) Bernhard E. J.; McKenna, W. G.; Hamilton, A. D.; Sebti, S. M.; Qian, Y.; Wu, J. M.; Muschel. R. J. *Cancer Res.* **1998**, *58*, 1754−1761.
(7) Leonard, D. M. *J. Med. Chem.* **1997**, *40*, 2971−2990.

10.1021/jo020299z CCC: $22.00
Published on Web 10/09/2002

arteminolide,[8] 8-acetylarteminolide, and arteminones[9] as inhibitors of FPTase, which were isolated from the *Artemisia sylvatica* Maxim (Compositae). Members of the *Artemisia* genus are important medicinal plants found throughout the world.[10] Artemisinin[11] is well-known as an antimalarial agent, which was isolated from *A. annua* L. Isolated compounds are sesquiterpene lactones which exhibit a wide range of biological activities.[12]

To evaluate potency, selectivity, and biological properties of arteminolides, several experiments were carried out *in vitro*. Here, we report the isolation, elucidation, and modification of structure for arteminolides, and results of FPTase inhibitory activity and H-*ras*-transformed cell-based assay.

These results suggest that arteminolides are novel inhibitors of FPTase and could be used as antitumor agents against *ras*-mutated human cancers or a wide array of human cancers.

Results and Discussion

Isolation and Structure elucidation. The methanol extract of the dried aerial parts of *Atemisia argyi* was fractionated by silica gel flash chromatography eluting with 10% MeOH in chloroform. Active fractions were further purified by C-18 column chromatography and gel filtration (Sephadex LH-20). Finally, the colorless solid arteminolide A (**1**), B (**2**), C (**3**), and D (**4**) and artanomaloide (**5**), A (**6**), and C (**7**) (Figure 1) were obtained by preparative reverse phase HPLC (YMC J'sphere ODS-H80, 250 mm × 20 mm i.d. column).

The structure of compound **1** was determined by spectroscopic methods (NMR, MS, and IR). The physical and spectral data of the isolated compound were identical with those of reported values.[8] Therefore we renamed the known arteminolide as arteminolide A (**1**).

The structure of arteminolide B (**2**) was elucidated by interpretation of NMR, IR, UV, and mass spectral data. Analysis of HRFABMS ($[M + H]^+$, *m*/*z* 589.2875) and the ^{13}C NMR spectrum of arteminolide B (**2**) led to a molecular formula of $C_{35}H_{40}O_8$, which indicated 16 degrees of unsaturation (see Table 1 for ^1H and ^{13}C NMR spectral data). The mass data showed that compound **2** has 2 mass units more than compound **1**.

The ^{13}C NMR of arteminolide B (**2**) exhibited 35 carbons. Identification of the protons attached to a specific carbon was performed by the HMQC experiment and DEPT spectrum, which revealed carbon signals for six methyls, five methylenes, seven methines, four olefinic methines, four quaternary carbons, five nonprotonated olefinics, and four carbonyls. The NMR analyses showed that compound **2** has a different side chain at C-8 in comparison with that of arteminolide A (**1**), having the dimethylacryloyl group. The existence of the 3,3-dimethylacryloyl moiety shown in Figure 2 was determined by the chemical shifts of C-2″ (115.73 ppm), C-3″ (158.76 ppm), and H-2″ (5.48 ppm). The structure was confirmed by the correlations of an ester carbonyl carbon (164.28 ppm, C-1″) with H-8 (4.87 ppm) and methyl groups with the carbons at C-2″ and C-3″ in the HMBC spectrum. The stereochemistry of the side chain was elucidated by the interaction between H-2″ and methyl group at C-4″ in the NOESY spectrum.

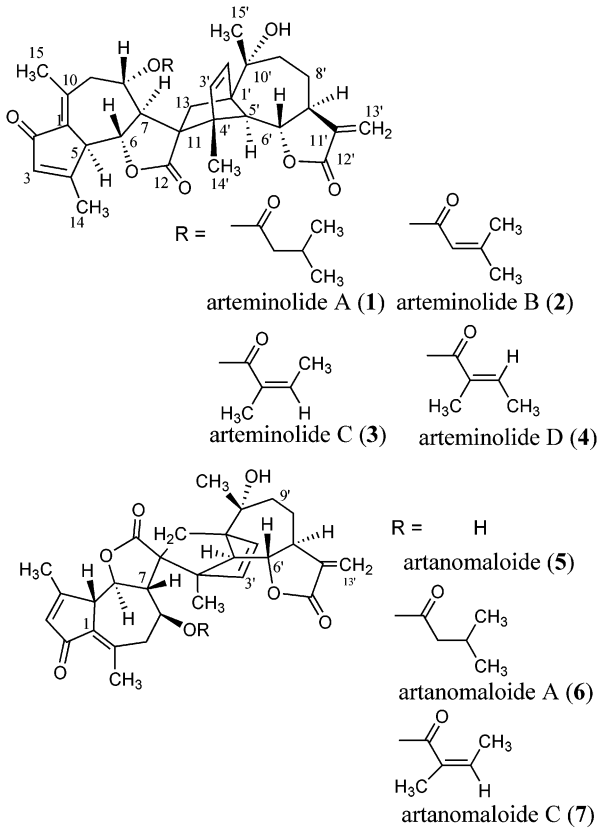

FIGURE 1. Structures of arteminolides and artanomaloides.

In the HRFABMS analyses of compounds **3** and **4**, molecular weight gave *m*/*z* 589.2796, which corresponded to a molecular formula of $C_{35}H_{40}O_8$. The results indicated that the compounds have the same molecular formula as arteminolide B (**2**). NMR experiments revealed that the position of the methyl groups of arteminolide C (**3**) and D (**4**) differed from that of arteminolide B (**2**), having the methyl group at both C-2″ and C-3″.

Comparison of the NMR data of compounds **3** and **4** with that of arteminolide B (**2**) suggested that compounds **3** and **4** were connected to the angeloyl and trigloyl group by an ester bond between C-8 and C-1″, respectively. The structure was confirmed by the correlation of an ester carbonyl carbon C-1″ with H-8 in the HMBC spectrum. The configuration at the C-2″−C-3″ double bond of compounds **3** and **4** was determined by NOESY spectra. Compound **4** was assigned as the *cis*-geometry by the observation of NOESY correlations between two methyl groups. However, the NOESY spectrum of compound **3** did not show any interactions of the two methyl groups, therefore the configuration at C-2″−C-3″ of compound **3** was assigned as the *trans*-geometry.

In analysis of HRFABMS ($[M + H]^+$) for compound **5**, molecular weight gave *m*/*z* 507.2386 which corresponded

(8) Lee, S. H.; Kim, M. J.; Bok, S. H.; Lee, H.; Kwon, B. M. *J. Org. Chem*. **1998**, *63*, 7111−7113.
(9) Lee, S. H.; Kang, H. M.; Song, H. C.; Lee, H.; Lee, U. C.; Son, K. H.; Kim, S. H.; Kwon, B. M. *Tetrahedron* **2000**, *56*, 4711−4715.
(10) Marco, J. A. *Studies in Natural Products Chemistry*; Elsevier: New York, 1990; pp 201−265.
(11) Haynes, R. K.; Vonwiller, S. C. *Acc. Chem. Res*. **1997**, *30*, 73−79.
(12) Robles, M.; Aregullin, M.; West, J.; Rodriguez, E. *Planta Med*. **1995**, *61*, 199−203.

TABLE 1. NMR Data of Arteminolide B (2) (500 MHz, in $CDCl_3$)

atom no.	δ_C	δ_H	HMBC (C→H)
1	133.96		3, 6, 9, 15
2	194.81		3
3	137.64	6.19 (dd, 1.5, 1.6)	1, 5, 14
4	170.06		3
5	52.06	3.26 (d, 10.3)	4, 6
6	80.21	4.03 (dd, 10.7, 9.8)	1, 5, 7
7	59.69	2.70 (dd, 11.3, 10.7)	6, 8, 11
8	67.31	4.77 (ddd, 10.7, 10.7, 2.4)	7
9	44.69	2.47 (dd, 13.2, 10.3)	1, 8, 10, 15
		2.35 (dd, 13.2, 2.3)	
10	144.12		
11	61.34		7, 3′, 5′, 14′
12	178.46		13
13	40.16	2.56 (d, 11.7),	1′, 2′, 10′, 12
		1.92 (d, 11.5)	
14	20.42	2.32 (s)	3, 4, 5
15	20.63	2.42 (s)	1, 9, 10
1′	62.91		2′, 4′, 5′
2′	137.64	5.73 (d, 5.9) 1′, 3′	1′, 3′
3′	135.93	5.82 (d, 5.4)	1′, 2′
4′	58.11		
5′	66.93	3.03 (d, 10.3)	1′, 2′, 6′
6′	79.10	3.97 (dd, 10.3, 9.8)	
7′	43.15	3.29 (m)	5′, 13′
8′	23.67	2.23 (m)	
		1.41 (m)	
9′	34.78	1.74 (ddd, 15.1, 8.8, 2.0)	15′
		1.83 (ddd, 15.1, 10.3, 7.8)	
10′	72.66		15′
11′	140.63		12′
12′	170.29		13′
13′	118.67	6.06 (d, 3.4)	7′, 12′
		5.32 (d, 3.4)	
14′	17.03	1.47 (s)	11, 3′, 4′, 5′
15′	29.67	1.26 (s)	1′, 9′, 10′
1″	164.28		8, 2″
2″	115.73	5.48 (dd, 1.5, 1.0)	
3″	158.76		4″, 5″
4″	20.32	2.21 (d, 1.0)	2″
5″	27.54	1.90 (d, 1.1)	2″

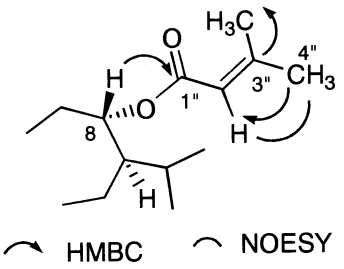

FIGURE 2. Partial structure of compound **3**.

to a molecular formula of $C_{30}H_{34}O_7$. Comparison of the ^1H and ^{13}C NMR spectrum of compound **5** with that of 8-acetylartanomaloide[13] suggested that artanomaloide (**5**) did not have any side chain at the C-8 position.

Arteminolides and artanomaloides are the products of Diels−Alder reactions between dienophile and diene as shown in Figure 3. NMR analyses (COSY, HMQC, and HMBC) revealed that the configuration at the cyclopentenyl ring (C-1′−C-5′) of arteminolide differed from that of artanomaloide, having a deshielding chemical shift at H-5′ (δ_H 3.06) of arteminolide C (**3**) in comparison with at H-5′ (δ_H 2.04) of artanomaloide C (**7**). Structures of

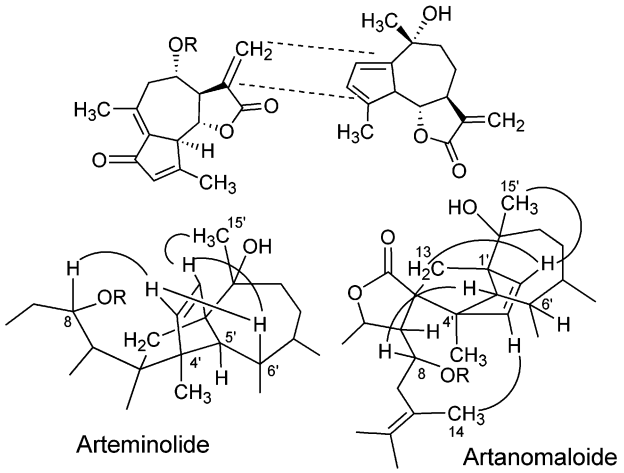

FIGURE 3. Regiochemistry of arteminolide and artanomaloide.

the regioisomers were also elucidated by the NOE experiments. The correlations between H-2′, 3′ and H-6, and also H-8 were observed in the NOESY spectrum of arteminolides. In the NOESY spectrum of artanomaloides, the across signals were not detected; however, between H-2′ and H-13, and H-3′ and H-14 correlations were observed. Also a new signal between H-8 and H-5′ was shown in the NOESY spectrum of artanomaloides (Figure 3).

Analyses of HRFABMS ($[M + H]^+$) for compounds **6** and **7** indicated that the molecular weights were *m*/*z* 591.2903 and 589.2787, which corresponded to a molecular formula of $C_{35}H_{42}O_8$ and $C_{35}H_{40}O_8$, respectively. The results indicated that compound **6** and **7** have the same molecular formula as arteminolide A (**1**) and C (**3**), respectively. NMR experiments (Table 2) of compound **6** revealed that the isovaleryl moiety was connected by an ester bond between C-8 of **5** and C-1″ of the isovaleryl group, which was confirmed by the chemical shifts at H-8 from 3.88 to 5.02 ppm and the cross signals between H-8 and C-1″ (172.17 ppm) in the HMBC spectrum.

Sesquiterpene lactones are a class of natural sesquiterpenoids that is chemically distinct from other members of the group though the presence of a γ-lactone system. Sesquiterpene lactones have antitumor activity, but their considerable cytotoxicity has so far prevented any useful medicinal application.[14] Arteminolide also possesses an α-methylene-γ-lactone group. To see whether the α-methylene-γ-lactone group of arteminolide was involved in the inhibition of FPTase, hydrogenation of arteminolide C (**3**) was performed with H_2/Pd-c in THF and arteminolide C′ (**8**) was purified by HPLC. The structure of the hydrogenated compound was established by comparison of spectroscopic data with that of arteminolide C (**3**). The molecular formula $C_{35}H_{44}O_8$ was obtained from the analyses of HRFABMS ($[M + H]^+$ 593.2874) for the hydrogenated compound, which means that two double bonds are reduced in this reaction. In the ^1H NMR study of **8**, it was found that the doublet signals of α-methylene-γ-lactone (H-13′at δ_H 5.31 and 6.05) disappeared and two new doublet methyl peaks were observed at δ_H 1.16 (J =

(13) Jakupovic, J.; Chen, Z. L.; Bohlmann, F. *Phytochemistry* **1987**, *26*, 2777−2779.

(14) Harborne, J. B. *Pytochemical Dictionary*; Taylor & Francis: Basingstoke, UK, **1993**, 599−644.

TABLE 2. NMR Data of Artanomaloide A (6) (500 MHz, in $CDCl_3$)

atom no.	δ_C	δ_H	HMBC (C→H)
1	134.17		3, 6, 9, 15
2	194.77		3
3	136.16	6.19 (brs)	5, 14
5	170.87		3, 5
5	50.31	3.49 (d, 9.8)	3, 7
6	79.17	3.71 (dd, 10.3, 9.8)	5, 7
7	56.65	2.98 (dd, 10.3, 10.3)	
8	65.10	5.02 (ddd, 10.3, 10.3, 2.0)	7
9	43.79	2.77 (dd, 13.2, 10.3)	15
		2.32 (dd, 13.2, 2.0)	
10	143.56		15
11	60.02		7, 3′, 5′, 14′
12	176.24		13
13	36.53	2.34 (d, 12.0),	2′,
		1.56 (d, 12.0)	
14	20.28	2.31 (brs)	
15	20.00	2.42 (s)	
1′	63.20		2′, 3′, 6′, 15′
2′	131.77	5.80 (d, 5.7)	13, 5′, 14′
3′	142.88	6.40 (d, 5.7)	14′
4′	57.30		14′
5′	66.34	1.98 (d, 9.8)	
6′	79.53	4.18 (dd, 9.8, 9.8)	
7′	43.28	3.06 (m)	5′, 13′
8′	23.70	2.19 (m)	6′
9′	34.85	1.46 (m)	15′
		1.83 (m)	
10′	72.56		15′
11′	140.86		12′
12′	170.29		13′
13′	119.34	6.11 (d, 3.4)	
		5.38 (d, 2.9)	
14′	14.56	1.56 (s)	
15′	29.80	1.29 (s)	
1″	172.17		8, 3″
2″	43.46	2.21 (m)	4″, 5″
		2.04 (m)	
3″	25.82	2.04 (m)	4″, 5″
4″	22.30	0.96 (d, 6.4)	
5”	22.16	0.93 (d, 6.4)	

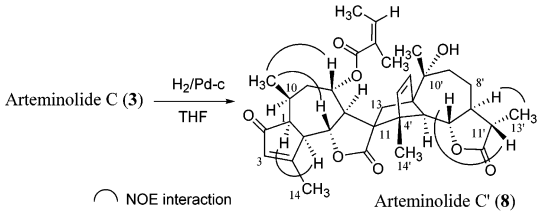

FIGURE 4. Reduction of arteminolide C (**3**).

6.8 Hz) and 1.09 (J = 7.3 Hz). In the ^{13}C NMR study of **8**, three quarternary olefinic peaks at δ_C 134.12, 143.87, and 140.63 also disappeared. The results suggested that the C-1−C-10 double bond of compound **3** was also hydrogenated under the reaction conditions (Figure 4). Stereochemistry of the reduced product was assigned by the NOE experiments.

***In Vitro* Enzyme Assay of FPTase and Kinetics.** FPTase assays were done with use of a scintillation proximity assay (SPA) kit following the protocol described by the manufacturer except that a biotinylated substrate peptide containing the Ki-Ras carboxyl-terminal sequence was used. The C-terminal peptide of Ki-Ras (Biotin-KKKSKTKCVIM) was synthesized by solid-phase peptide synthesis. FPTase activity was determined by measuring transfer of [^{3}H]-farnesyl from [^{3}H]-farnesyl pyrophosphate to Biotin-KKKSKTKCVIM. Arteminolide series inhibited a recombinant human FPTase with IC_{50} values of 0.76 (**2**), 0.95 (**3**), and 1.1 μM (**4**). However, artanomaloides, regioisomers of arteminolide, inhibited the enzyme with IC_{50} values of 200 (**5**), 105 (**6**), and 150 μM (**7**). Reduced compound **8** (arteminolide C′) also inhibited FPTase with an IC_{50} value of 1.0 μM. This result showed that inhibitory activity of the compound is very similar to that of arteminolide C (**3**) and that the α-methylene-γ-lactone group did not affect the inhibition of FPTase. Arteminolides and artanomaloides did not inhibit rat squalene synthase ($IC_{50} \gg 200$ μM) and recombinant rat geranyl-geranyl protein transferase I ($IC_{50} \gg 200$ μM).

To determine whether the inhibitors competed with FPP or K-Ras peptides, a kinetic analysis was performed by scintillation proximity assay with highly purified recombinant FPTase. From the experiments, it was found that the inhibition of FPTase by arteminolide was competitive with respect to FPP and noncompetitive with respect to K-Ras peptide. From plots of the slope of the double-reciprocal lines versus inhibitor concentration, the K_i values of arteminolide D (**4**) for FPTase inhibition were calculated to be 1.8 μM with respect to FPP and 1.6 μM with respect to the K-Ras peptide.

H-Ras Processing and Growth Inhibition in H-*ras*-Transformed NIH3T3 Cells. To determine the potency of the FPTase inhibitors in cells, we evaluated the effect of the isolated compounds on the growth of H-*ras*-transformed cell lines. GI_{50} values of arteminolide C and C′ were 1.5 and 12 μM against H-*ras*-transformed NIH3T3, respectively. However, the compounds inhibited the growth of NIH3T3 cells with GI_{50} values of 5.5 and 35 μM, respectively. These results showed that the FPTase inhibitors more strongly inhibited the growth of transformed cells than normal cells and the modification of the α-methylene-γ-lactone group had a strong effect on the cytotoxicity of the compounds against cells. To examine the effect of arteminolides on Ras processing in H-*ras*-transformed cell lines, arteminolide C (**3**) was treated in the cells. After treatment of the compound in cell, membrane fractions were obtained from cell lysates and then resolved by SDS-PAGE. The amount of processed H-Ras protein was determined by immunoblotting, using an antibody specific for H-Ras. In the presence of the inhibitor, the amount of the H-Ras protein in the membrane factions was decreased (Figure 5).

Experimental Section

Isolation. Leaves of *A. argyi* were collected in 2000, near Incheon City, Korea, and identified by Professor K. Bae, School of Pharmacy, Chungnam National University. Leaves of *A. argyi* (10 kg) were extracted with $CHCl_3$ (2 × 20 L). The combined extract was concentrated, and the dark residue was subjected to silica gel flash chromatography with $CHCl_3$/MeOH solvent pairs. Fractions were monitored by FPTase inhibition activity and silica gel TLC ($CHCl_3$−MeOH, 9:1). The active fractions ($CHCl_3$−MeOH, from 9:1 to 8:2) were subjected to C18 column chromatography with aqueous MeOH. The two fractions eluted with 70% and 80% MeOH were shown to have strong inhibition activity against rat FPTase and were collected and further purified by chromatography on a Sephadex LH-20 column eluting with MeOH. Final purification of arteminolides A−D (**1**−**4**) and artanomaloides A and B (**5**−**7**) was accomplished by ODS-HPLC with 80% MeOH to yield compounds.

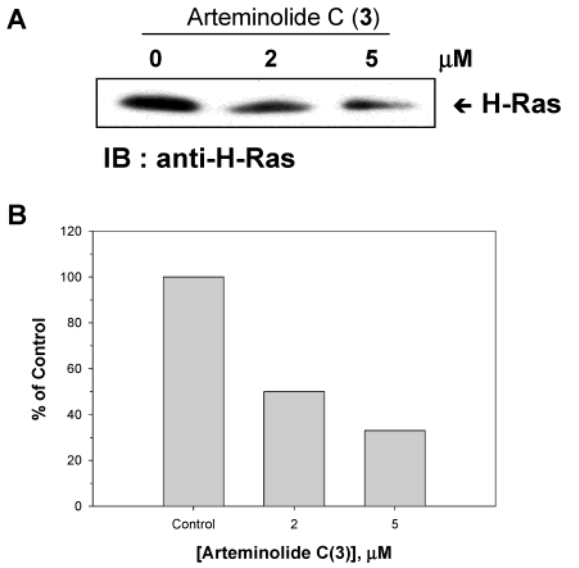

FIGURE 5. Inhibition of H-Ras processing in H-*ras*-transformed cells by arteminolide C (**3**). Lane 1, control; Lane 2, 2 μM; Lane 3, 5 μM.

Arteminolide B (2): mp 210−212 °C; UV (MeOH) λ_{max} 220 (ϵ = 5964), 254 (ϵ = 6432) nm; $[\alpha]^{25}_D$ +10° (*c* 0.11, MeOH); IR (KBr) ν_{max} 3600−3400, 2927, 1758, 1687, 1650, 1617, 1230, 1147, and 908 cm^{-1}; DEI *m*/*z* (rel intensity, %) 342 (6.2), 242 (28.7), 228 (13.5), 83 (69.5), 55 (30.2), 44 (100); DCI *m*/*z* (rel intensity, %) 589 (1.8), 343 (99.6), 243 (79.9), 229 (100).

Arteminolide C (3): mp 211−215 °C; UV (MeOH) λ_{max} 215 (ϵ = 5904), 253 (ϵ = 6511) nm; $[\alpha]^{25}_D$ +5° (*c* 0.11, MeOH); IR (KBr) ν_{max} 3600−3400, 2925, 1760, 1697, 1650, 1617, 1230, 1147, and 908 cm^{-1}; DEI *m*/*z* (rel intensity, %) 342 (22.7), 242 (62.7), 228 (25.0), 83 (96.7), 55 (100); DCI *m*/*z* (rel intensity, %) 589 (6.8), 343 (80.6), 243 (79.9), 229 (100).

Arteminolide D (4): mp 200−205 °C; UV (MeOH) λ_{max} 216 (ϵ = 5901), 253 (ϵ = 6551) nm; $[\alpha]^{25}_D$ +50° (*c* 0.11, MeOH); IR (KBr) ν_{max} 3600−3400, 2927, 1768, 1697, 1650, 1617, 1230, 1147, and 908 cm^{-1}; DEI *m*/*z* (rel intensity, %) 342 (36.7), 242 (100), 228 (22.0), 83 (56.8), 55 (51.7); DCI *m*/*z* (rel intensity, %) 589 (8.8), 343 (90.6), 243 (79.9), 229 (100).

Artanomaloide (5): mp 165−169 °C; UV (MeOH) λ_{max} 205 (ϵ = 5804), 257 (ϵ = 6651) nm; $[\alpha]^{25}_D$ −40°(*c* 0.12, MeOH); IR (KBr) ν_{max} 3600−3400, 2936, 1760, 1669, 1636, 1612, 1221, 1147, and 908 cm^{-1}; DEI *m*/*z* (rel intensity, %) 260 (26.7), 242 (42.7), 83 (22.0), 55 (100); DCI *m*/*z* (rel intensity, %) 507 (7.5), 303 (30.6), 247 (12.4), 243 (79.9), 229 (100).

Artanomaloide A (6): mp 195−196 °C; UV (MeOH) λ_{max} 215 (ϵ = 5904), 252 (ϵ = 6451) nm; $[\alpha]^{25}_D$ −25° (*c* 0.12, MeOH); IR (KBr) ν_{max} 3600−3400, 2927, 1766, 1687, 1650, 1617, 1230, 1147, and 908 cm^{-1}; DEI *m*/*z* (rel intensity, %) 344 (16.7), 242 (100), 228 (65.1), 83 (22.0), 55 (51.7); DCI *m*/*z* (rel intensity, %) 591 (6.2), 345 (99.6), 247 (43.4), 243 (79.9), 229 (100).

Artanomaloide C (7): mp 190−193 °C; UV (MeOH) λ_{max} 215 (ϵ = 5914), 253 (ϵ = 6581) nm; $[\alpha]^{25}_D$ −45° (*c* 0.11, MeOH); IR (KBr) ν_{max} 3600−3400, 2929, 1765, 1698, 1651, 1616, 1230, 1147, and 908 cm^{-1}; DEI *m*/*z* (rel intensity, %) 342 (26.7), 242 (100), 228 (52.3), 83 (22.0), 55 (100); DCI *m*/*z* (rel intensity, %) 589 (9.8), 343 (60.6), 247 (43.4), 243 (100), 229 (75.3).

Reduction of the α-Methylene-γ-Lactone Group of Arteminolide C (3). For reduction of the α-methylene-γ-lactone group, arteminolide C (**3**) was dissolved in THF and stirred at room temperature. Then, palladium on charcoal was added to the solution and stirred at room temperature under a hydrogen atmosphere for 30 min. The resulting mixture was concentrated in a vacuum evaporator and purified by HPLC to give arteminolide C′ (**8**).

Arteminolide C′ (8): mp 168−175 °C; UV (MeOH) λ_{max} 217 nm; $[\alpha]^{25}_D$ +35° (*c* 0.15, MeOH); IR (KBr) ν_{max} 3600−3400, 2915, 1730, 1717, 1655, 1617, 1228, 1147 and 908 cm^{-1}; DEI *m*/*z* (rel intensity, %) 344 (12.7), 244 (32.3), 232 (25.0), 83 (96.7), 55 (100); ^{1}H NMR in $CDCl_3$ δ 2.73 (1H, dd, *J* = 5.9, 5.9 Hz), 6.05 (3H, dq, *J* = 1.5, 1.5 Hz), 2.96 (5H, dd, *J* = 10.1, 7.3 Hz), 4.40 (6H, dd, *J* = 10.7, 10.1 Hz), 2.75 (7H, dd, *J* = 10.7, 10.7 Hz), 5.12 (8H, ddd, *J* = 10.7, 7.3, 3.9 Hz), 2.11 (9H, m), 1.57 (9H, m), 2.45 (10H, m), 2.61 (13H, d, *J* = 11.2 Hz), 1.76 (13H, d, *J* = 11.2 Hz), 2.33 (14H, s), 1.07 (15H, d, *J* = 7.3 Hz), 5.67 (2′H, d, *J* = 5.4 Hz), 5.95 (3′H, d, *J* = 5.4 Hz), 3.07 (5′H, d, *J* = 9.8 Hz), 3.96 (6′H, dd, *J* = 9.8, 9.8 Hz), 2.34 (7′H, m), 2.04 (8′H, m), 1.30 (8′H, m), 1.82 (9′H, m), 1.78 (9′H, m), 2.00 (11′H, m), 1.16 (13′H, d, *J* = 6.8 Hz), 1.47 (14′H, s), 1.16 (15′H, s), 6.75 (3″H, qq, *J* = 6.8, 1.5 Hz), 1.79 (4″H, dq, *J* = 6.8, 1.5 Hz), 1.81 (5″H, br q, *J* = 1.5 Hz); ^{13}C NMR in $CDCl_3$ δ 54.36 (C-1), 207.74 (C-2), 132.46 (C-3), 178.73 (C-4), 54.28 (C-5), 78.40 (C-6), 54.59 (C-7), 69.90 (C-8), 38.08 (C-9), 28.07 (C-10), 61.45 (C-11), 178.90 (C-12), 41.42 (C-13), 17.77 (C-14), 20.61 (C-15), 62.67 (C-1′), 136.95 (C-2′), 136.98 (C-3′), 57.84 (C-4′), 66.45 (C-5′), 79.58 (C-6′), 46.39 (C-7′), 24.67 (C-8′), 35.30 (C-9′), 72.62 (C-10′), 42.84 (C-11′), 179.00 (C-12′), 12.93 (C-13′), 16.48 (C-14′), 29.57 (C-15′), 166.05 (C-1″), 129.01 (C-2″), 137.78 (C-3″), 14.40 (C-4″), 12.05 (C-5″).

***In Vitro* Enzyme Assay of FPTase and Kinetics.** FPTase assays were done with a scintillation proximity assay (SPA) kit following the protocol described by the manufacturer (Amersharm Bioscience), except that a biotinylated substrate peptide containing the Ki-Ras carboxyl-terminal sequence was used. The C-terminal peptide of Ki-Ras (Peptron, Taejon in Korea) has the sequence Biotin-KKKSKTKCVIM. Recombinant rat FPTase was kindly provided by Patrick J. Casey (University of Duke, USA). FPT activity was determined by measuring the transfer of [^{3}H]-farnesyl from [^{3}H]-farnesyl pyrophosphate to Biotin-KKKSKTKCVIM. Typical reaction mixtures (100 μL total) contained 50 mM HEPES, pH 7.5, 30 mM $MgCl_2$, 20 mM KCl, 5 mM DTT, 0.01% Triton X-100, 150−250 nM [^{3}H]farnesyl pyrophosphate (60 μM, 1 Ci/μL), 25−50 ng (approximately 2.5−5 nM) of recombinant rat FPTase or 10 μL of partially purified Q-Sepharose-derived FPTase, the indicated concentration of arteminolides or dimethyl sulfoxide (DMSO) vehicle control (10%, v/v, final), and 10−200 nM Biotin-KKKSKTKCVIM. After 60 min incubation in a water bath at 37 °C, reactions were stopped by adding 150 μL of STOP/bead reagent into each tube/well. Radioactivities were mixed with vortex and let stand for 30 min at room temperature. Samples were measured in a Wallac 1450 microbeta TRILUX liquid scintillation counter. Percent inhibition was calculated relative to the DMSO vehicle control. The GGPTase-1 assay was essentially identical with the FPTase assay described above with [^{3}H]-geranylgeranyl pyrophosphate (100 nM) instead of farnesyl pyrophosphate.[15]

Cell Culture and Growth Inhibition Assays. H-*ras*-transformed NIH3T3 cells were grown in DMEM supplemented with 10% heat-inactivated FBS at 37 °C under a humidified atmosphere of 5% CO_2 and 95% air in an incubator. Cells (5000 cells/well) were seeded in 96-well microtiter plates in DMEM containing 10% FBS. After 24 h, cells were replenished with fresh complete medium containing either a test compound or 0.1% DMSO. After incubation for 48 h, proliferation reagent WST-1 (Roche Molecular Biochemicals) was added to each well. The amount of WST-1 formazan produced was measured at 450 nm with an ELISA Reader (Bio-Rad).[16]

The Processing of H-Ras in H-*ras*-Transformed NIH3T3 Cells. An H-Ras processing assay was performed as described previously by Garcia et al.[17] H-*ras*-transformed NIH3T3 cells were seeded in DMEM containing 10% FBS in a T25 culture

(15) Agnew, W. S. *Methods Enzymol.* **1985**, *110*, 359−373.
(16) Kim, H. M.; Han, S. B.; Kim, S. M.; Kang, J. S.; Oh, G. T.; Hong, D. H. *Toxicol. Pharmacol. Methods* **1996**, *36*, 163−169.
(17) Garcia, A. M.; Rowell, C.; Ackerman, K.; Kowalczyk, J. J.; Lewis, M. D. *J. Biol. Chem.* **1993**, *268*, 18415−18418.

flask. One day after seeding, cells were replenished with fresh complete medium containing compound **3** or 0.1% DMSO. After 48 h, cell monolayers were washed twice with ice-cold TBS (150 mM NaCl and 50 mM Tris, pH 7.4), scraped, and pelleted by centrifugation at 800 rpm for 5 min at 4 °C. A cytosolic fraction was prepared by resuspending the cell pellet in 1.0 mL of MOPS buffer (20 mM MOPS, pH 7.4, 5 mM $MgCl_2$, 2 mM EDTA, 10% (v/v) glycerol, plus protease and phosphatase inhibitors) containing 0.05% (w/v) saponin and incubating on ice for 30 min. Cell ghosts were collected by centrifugation at 13 000 rpm for 10 min at 4 °C in a refrigerated bench microcentrifuge. The pellet was washed three times with ice-cold TBS and an enriched membrane fraction was prepared by extracting the cell pellet for 20 min on ice with 200−500 μL of 1.0% (w/v) CHAPS in MOPS buffer. Insoluble cellular debris was pelleted by centrifugation at 13 000 rpm at 4 °C. The protein concentration of the membrane-enriched fraction was determined by Bradford assay. Proteins (30 μg) of each cell extract were separated by SDS-PAGE in 12% acrylamide gels. Gels were blotted onto a PVDF membrane (Bio-Rad) and blots were blocked with TBST (50 mM Tris-HCl, pH 7.6, 150 mM NaCl and 0.1% Tween 20) containing blocking reagents (Roche Molecular Biochemicals) for 1 h. Proteins were probed with a monoclonal anti-H-Ras antibody, visualized with chemiluminescence POD reagents (Roche Molecular Biochemicals) and then exposed to chemiluminescence film.

Acknowledgment. This research was financially supported by a grant (code: PF002107-00) from the Plant Diversity Research Center of 21st Century Frontier Research Program and by a grant (No. 2000-2-21100-003-3) from the Basic Research Program of the Korea Science & Engineering Foundation.

Supporting Information Available: ^{1}H NMR, ^{13}C NMR, ^{1}H−^{1}H COSY, HMQC, mass, IR, and HMBC spectral data and spectra for arteminolides and artanomaloides, and ^{1}H NMR of artanomaloide (**5**) and arteminolide (**8**). This material is available free of charge via the Internet at http://pubs.acs.org.

JO020299Z